Electronic Supplementary Information

Experimental Section

Materials: Sodium hydroxide (NaOH), ammonium chloride (NH_4Cl), sodium sulfate (Na_2SO_4), ethylalcohol (C_2H_5OH), hydrochloric acid (HCl), sodium nitrite ($NaNO_2$, 99.0%), sodium salicylate ($C_7H_5O_3Na$), sodium nitroferricyanide dihydrate ($C_5FeN_6Na_2O\cdot 2H_2O$), sodium hypochlorite solution (NaClO), and p-dimethylaminobenzaldehyde ($C_9H_{11}NO$) were purchased from Aladdin Ltd. (Shanghai, Chain). Sulfuric acid (H_2SO_4), hydrogen peroxide (H_2O_2), sodium hypophosphite (NaH_2PO_2), and hydrazine monohydrate ($N_2H_4\cdot H_2O$) were bought from Beijing Chemical Corporation. (China). Titanium plate (TP) (thickness is 0.2 mm) was purchased from Qingyuan Metal Materials Co., Ltd (Xingtai, China) and treated with 2 M HCl for 30 minutes before hydrothermal reaction. All reagents used in this work were analytical grade and direct use without further purification.

Synthesis of P-TiO_2/TP and TiO_2/TP: Firstly, TP was cut into a small piece (2.0 × 4.0 cm^2) and sonicated in acetone, ethanol, and distilled water for 15 min, respectively. After then, TP was put into 30 mL of 5 M NaOH aqueous solution in 50 mL Teflon-lined autoclave. The autoclave was kept in an electric oven at 180℃ for 24 h. After the autoclave was cooled down naturally to room temperature, the sample was moved out, washed with deionized water and ethanol several times and dried at 60 ℃ for 10 min. Then the resultant $Na_2Ti_2O_5$/TP was immersed in 1 M HCl for 1 h in order to exchange Na^+ with H^+. As-prepared $H_2Ti_2O_5\cdot H_2O$/TP was rinsed with deionized water and ethanol several times and dried at 60 ℃ for 10 min. Subsequently, it was placed in a tube furnace with another 1 g of NaH_2PO_2 at the upstream position, with only 2 h of heating treatment at 500 °C under Ar atmosphere, then the P-TiO_2/TP was finally obtained. TiO_2/TP was synthesized using the same methods but without the addition of NaH_2PO_2 at annealing process.

Characterizations: XRD data were acquired by a LabX XRD-6100 X-ray diffractometer with a Cu Kα radiation (40 kV, 30 mA) of wavelength 0.154 nm (SHIMADZU, Japan). SEM measurements were carried out on a Gemini SEM 300 scanning electron microscope (ZEISS, Germany) at an accelerating voltage of 5 kV. XPS measurements were performed on an ESCALABMK II X-ray photoelectron spectrometer using Mg as the exciting source. The absorbance data of spectrophotometer was measured on UV-Vis spectrophotometer. TEM image was obtained from a

Zeiss Libra 200FE transmission electron microscope operated at 200 kV. EPR spectra were recorded on a Brüker EMX spectrometer at room temperature.

Electrochemical measurements: All electrochemical measurements were carried on the CHI660E electrochemical workstation (Shanghai, Chenhua) using a standard three-electrode setup. Electrolyte solution was Ar-saturated of 0.1 M Na_2SO_4 with 0.1 M NO_2^-, using P-TiO_2/TP (0.5 × 0.5 cm^2) as the working electrode, graphite rod as the counter electrode and an Ag/AgCl as the reference electrode. We use an H-type electrolytic cell separated by a Nafion 117 membrane which was protonated by boiling in ultrapure water for 2 h, then in H_2O_2 (5%) aqueous solution for 2 h, followed by 3 h in 0.5 M H_2SO_4, and finally for 6 h in water. All the potentials reported in our work were converted to reversible hydrogen electrode via calibration with the following equation: E (vs. RHE) = E (vs. Ag/AgCl) + 0.059 × pH + 0.197 V, and the presented current densities were normalized to the geometric area of the electrode.

Determination of NH_3: The concentration of produced NH_3 was determined by colorimetry (the obtained electrolyte was diluted 40 times) using the indophenol blue method.[1] In detail, a certain amount of electrolyte was taken out from the electrolytic cell and diluted to 4 mL to the detection range. Then, 50 μL oxidizing solution containing NaClO (4.5%) and NaOH (0.75 M), 500 μL coloring solution containing $C_7H_5O_3Na$ (0.4 M) and NaOH (0.32 M), and 50 μL catalyst solution $Na_2Fe(CN)_5NO{\cdot}2H_2O$ (1 wt%) were dropped into the collected electrolyte solution. After standing at room temperature for 1 h, the ultraviolet-visible (UV-Vis) absorption spectrum was measured. The concentration of NH_3 was determined using the absorbance at a wavelength of 660 nm. The concentration-absorbance curve was calibrated using the standard NH_4Cl solution with NH_3 concentrations of 0, 0.2, 0.5, 1.0, 2.0 and 5.0 ppm in 0.1 M Na_2SO_4 solution. The fitting curve ($y = 0.4432\ x + 0.0352$, $R^2 = 0.9998$) shows a good linear relation of absorbance value with NH_3 concentration.

Determination of N_2H_4: In this work, we used the method of Watt and Chrisp to determine the concentration of produced N_2H_4.[2] The chromogenic reagent was a mixed solution of 5.99 g $C_9H_{11}NO$, 30 mL HCl and 300 mL C_2H_5OH. In detail, 1 mL electrolyte was added into 1 mL prepared color reagent and standing for 15 min in the dark. The absorbance at 455 nm was measured to quantify the N_2H_4 concentration with a standard curve of hydrazine ($y = 0.6388\ x + 0.0605$, $R^2 = 0.9998$).

Calculations of the FE and NH_3 yield rate:

The amount of NH_3 (n_{NH3}) was calculated by the following equation:

$$n_{NH3} = [NH_3] \times V$$

FE of NH_3 formation was calculated by the following equation:

$$FE = (6 \times F \times [NH_3] \times V) / (M_{NH3} \times Q) \times 100\% \quad (1)$$

NH_3 yield rate is calculated using the following equation:

$$NH_3 \text{ yield rate} = ([NH_3] \times V) / (M_{NH3} \times t \times A) \quad (2)$$

Where F is the Faradic constant (96500 C mol^{-1}), $[NH_3]$ is the measured NH_3 concentration, V is the volume of electrolyte in the cathode compartment (35 mL), M_{NH3} is the molar mass of NH_3, Q is the total quantity of applied electricity; t is the electrolysis time (1 h) and A is the geometric area of catalyst (0.5 × 0.5 cm^2).

DFT calculation details: The density functional theory (DFT) calculations were conducted by plane-wave DFT implemented in the Vienna *Ab initio* Simulation Package (VASP). Potentials constructed with the full potential projector augmented wave (PAW) method were used for the elemental constituents.[3] The exchange correlation was treated with the generalized gradient approximation (GGA) Perdew-Burke-Ernzerhof (PBE) functional.[4] Spin polarization was also included. A (3 × 1) unit cell of TiO_2 (101) slab was constructed for the DFT calculations. The cell length was 10.45 Å × 11.35 Å for x and y direction. Two layers of TiO_2 were constructed along the z direction, with a vacuum layer of 20 Å. In each calculation, 500 eV cutoff energy and 2 × 2 × 1 K-mesh were chosen to achieve a convergence of 2 meV/atom. The convergence criteria were set to be the energy of 10^{-6} eV/atom and the force of 0.2 eV/nm for the electronic and ionic steps in relaxation, respectively. In the relaxation, the bottom layer was fixed while the upper layer was allowed to move. The Gibbs free energy of each structure was the DFT calculated energy added by the Gibbs free energy term. The former can be directly obtained from DFT while the latter was obtained by calculating the vibration frequency.

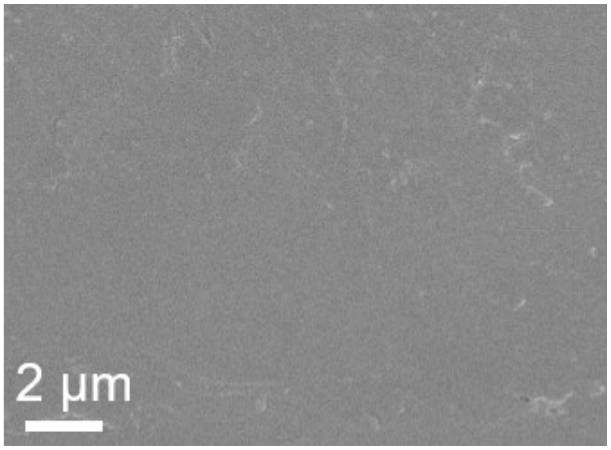

Fig. S1. SEM image of bare TP.

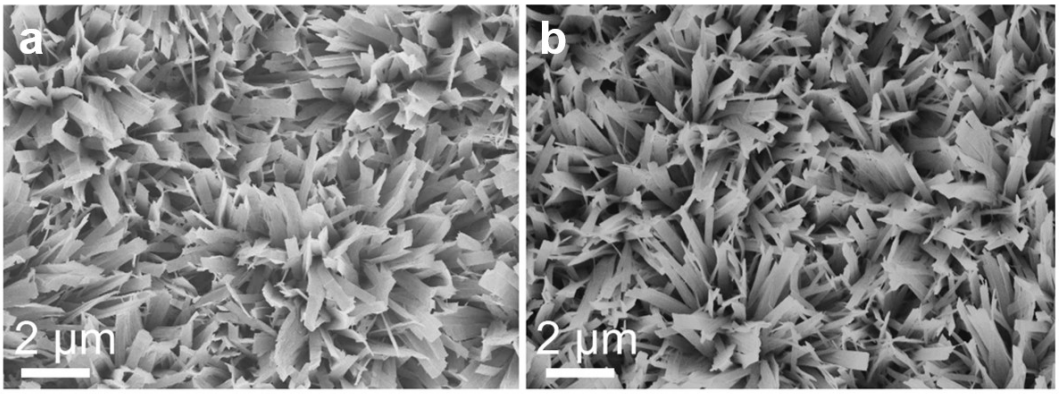

Fig. S2. SEM images of (a) $Na_2Ti_2O_5$/TP and (b) $H_2Ti_2O_5$/TP.

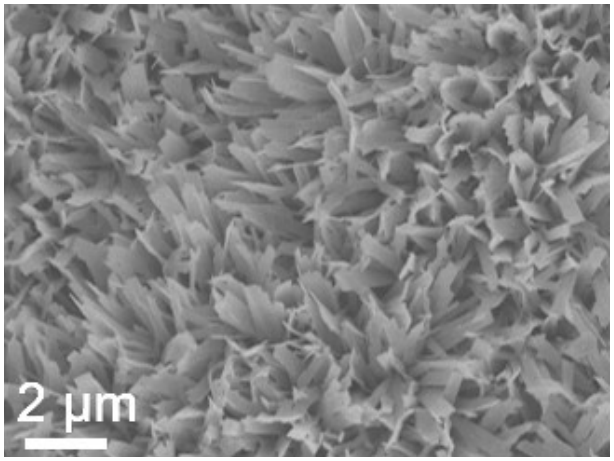

Fig. S3. SEM image of TiO_2/TP.

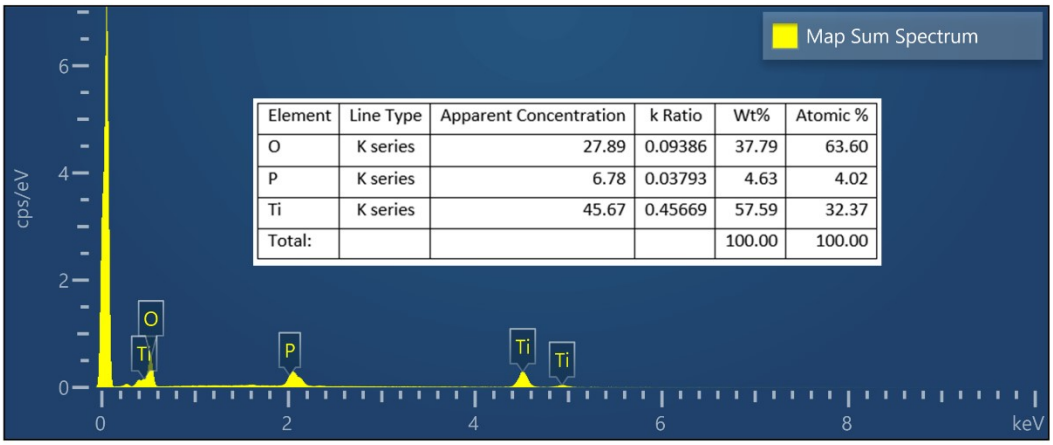

Element	Line Type	Apparent Concentration	k Ratio	Wt%	Atomic %
O	K series	27.89	0.09386	37.79	63.60
P	K series	6.78	0.03793	4.63	4.02
Ti	K series	45.67	0.45669	57.59	32.37
Total:				100.00	100.00

Fig. S4. EDX spectrum of P-TiO_2/TP.

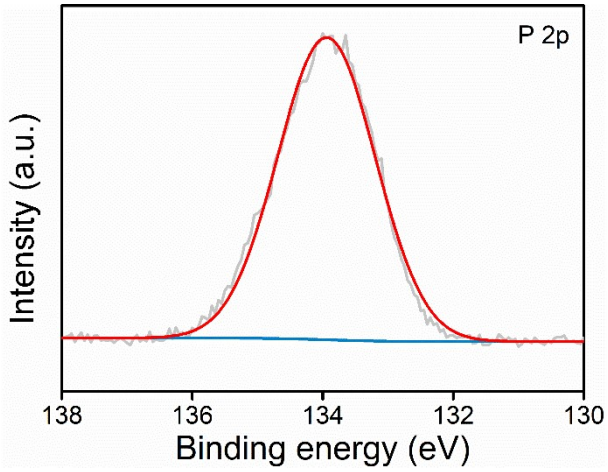

Fig. S5. XPS spectrum of P 2p for P-TiO_2.

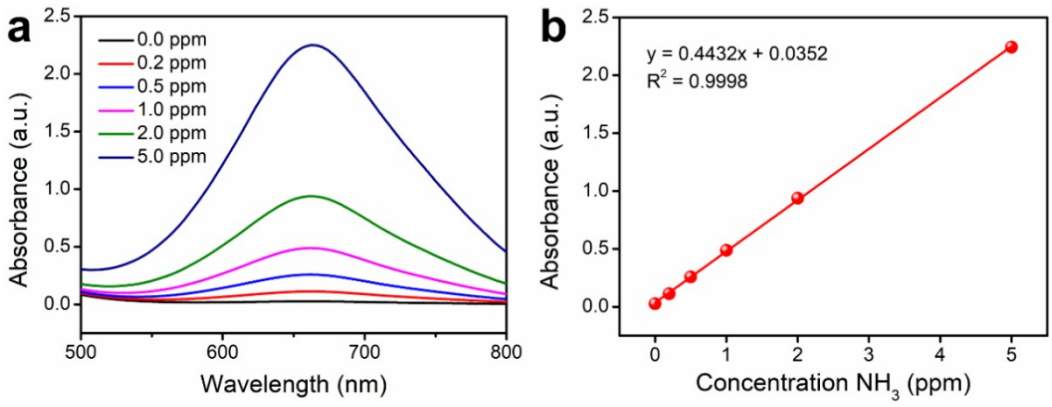

Fig. S6. (a) UV-Vis absorption spectra of indophenol assays kept with different concentrations of NH_3 after incubated for 1 h at room temperature. (b) Corresponding calibration curve used for calculation of NH_3 concentration.

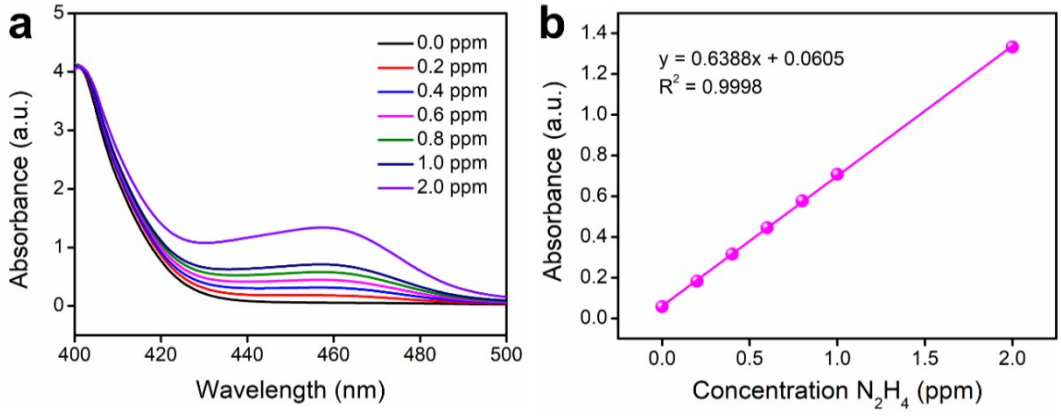

Fig. S7. (a) UV-Vis absorption spectra various N_2H_4 concentrations after incubated for 15 min at room temperature. (b) Corresponding calibration curve used for calculation of N_2H_4 concentration.

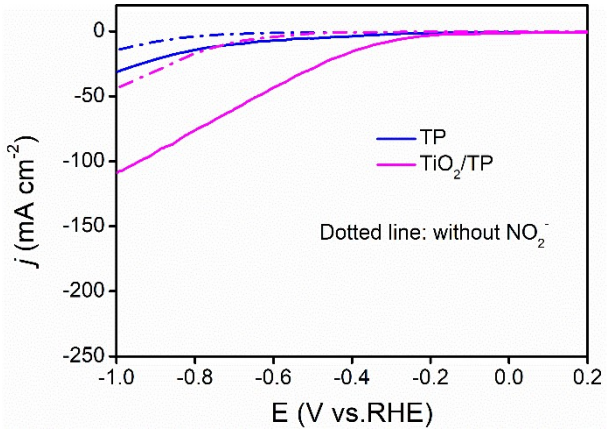

Fig. S8. LSV curves of TiO_2/TP and TP in 0.1 M Na_2SO_4 with and without 0.1 M NO_2^-.

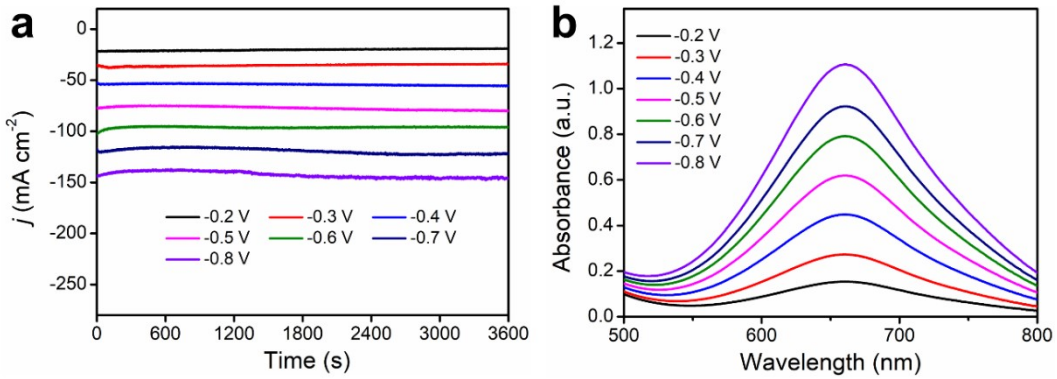

Fig. S9. (a) Chronoamperometry curves of P-TiO_2/TP at each given potential and (b) corresponding UV-Vis absorption spectra of the electrolytes for calculation of NH_3 concentration.

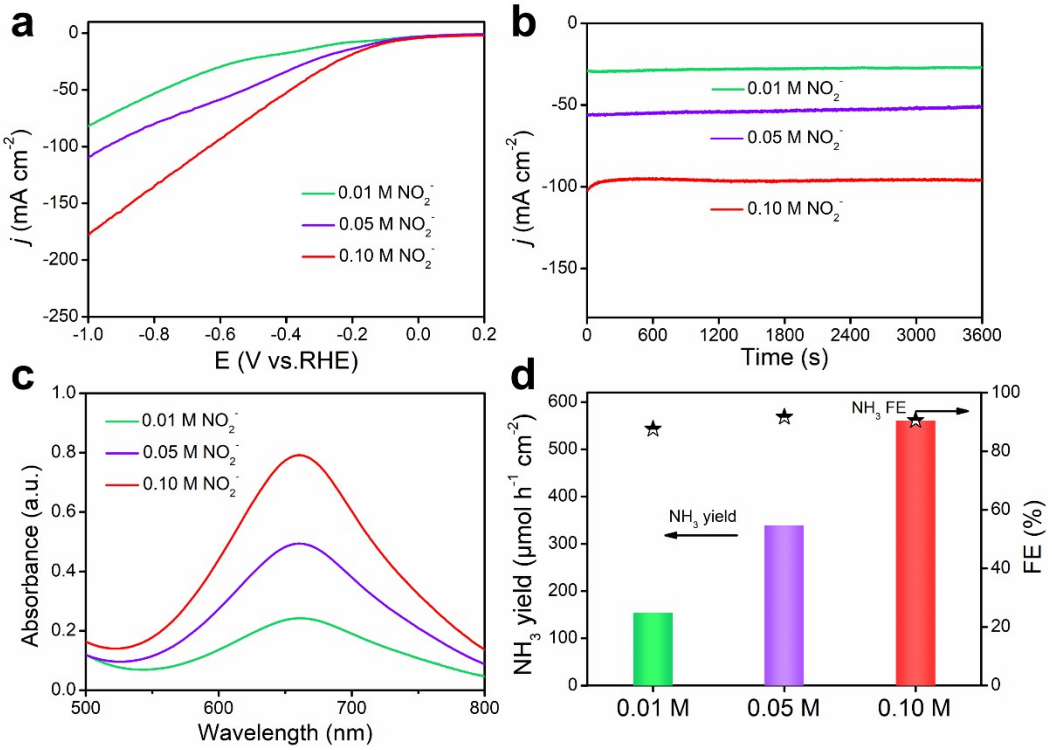

Fig. S10. (a) LSV curves, (b) Time-dependent current density curves, (c) corresponding UV-Vis absorption spectra, and (d) NH_3 yields and FEs in 0.1 M Na_2SO_4 with different NO_2^- concentrations.

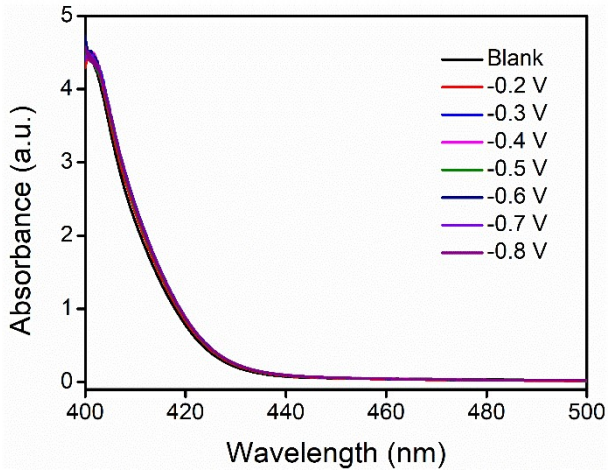

Fig. S11. (a) UV-Vis absorption spectra of the electrolytes estimated by the method of Watt and Chrisp for the calculation of N_2H_4 concentration.

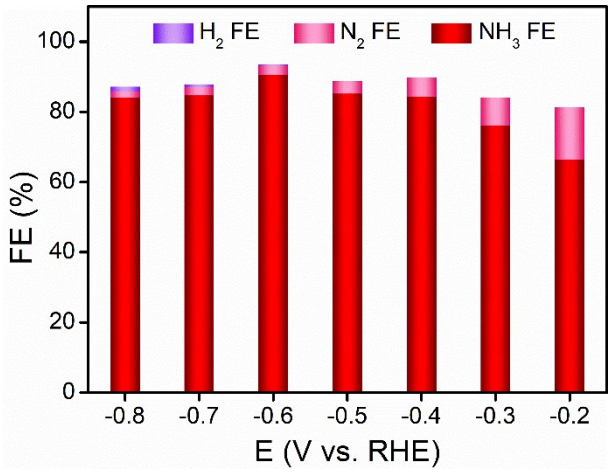

Fig. S12. FEs of NH_3, N_2, and H_2 of P-TiO_2/TP at different given potentials.

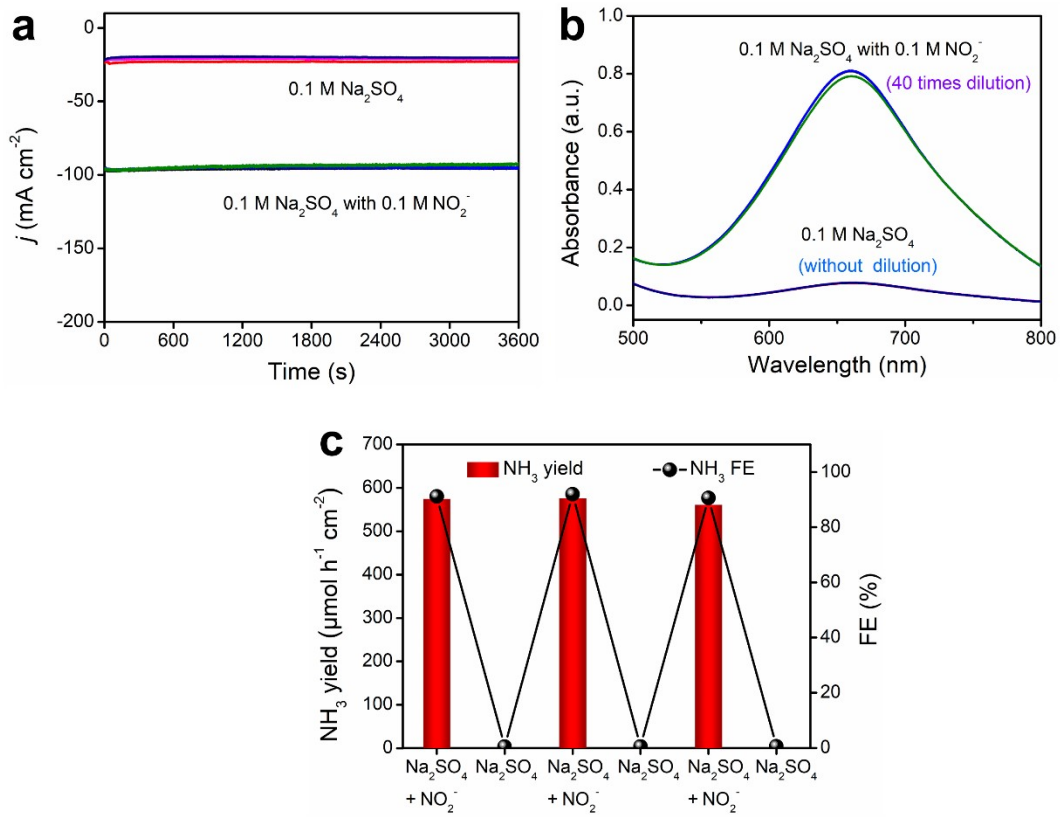

Fig. S13. (a) Time-dependent current density curves, (b) corresponding UV-Vis spectra, and (c) NH_3 yields and FEs of P-TiO_2/TP during the alternating cycles tests between NO_2^--containing and NO_2^--free 0.1 M Na_2SO_4 solution.

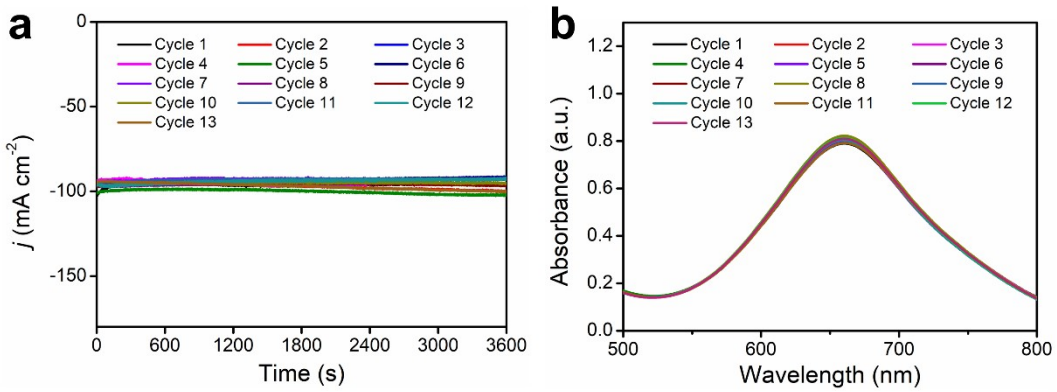

Fig. S14. (a) Chronoamperometry curves and (b) corresponding UV-Vis absorption spectra of P-TiO_2/TP for electrochemical catalytic production of NH_3 during cycling tests at –0.6 V.

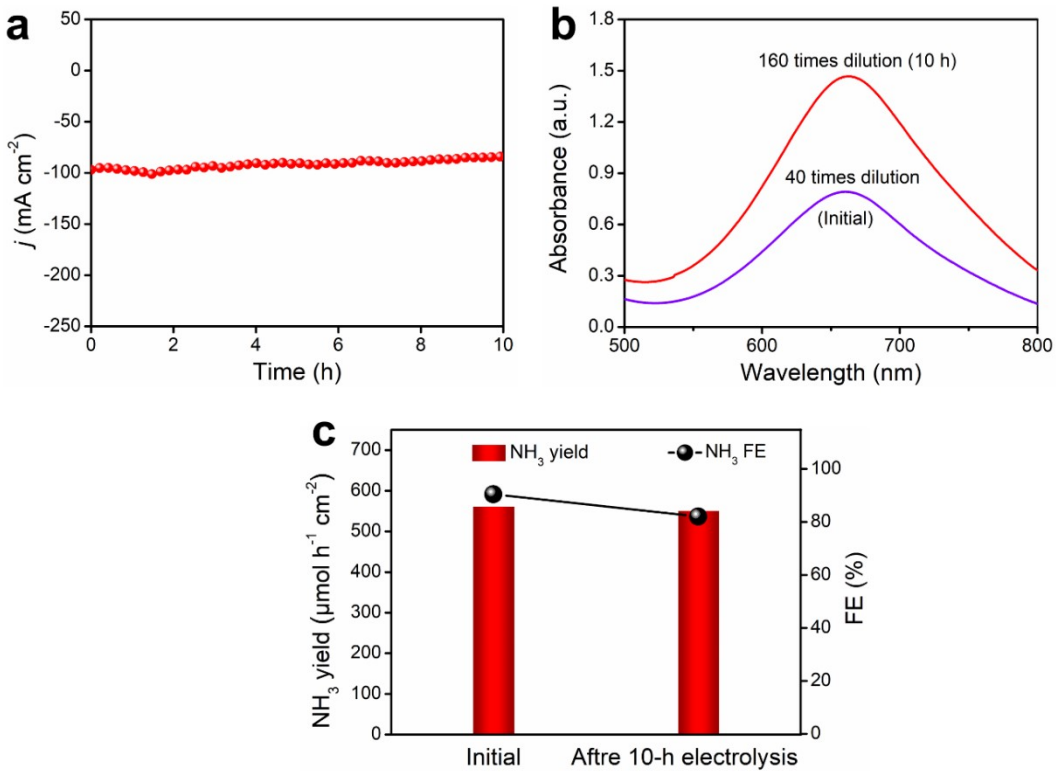

Fig. S15. (a) Chronoamperometry curve of P-TiO_2/TP at −0.6 V for 10 h. (b) Corresponding UV-Vis spectra and (c) NH_3 yields and FEs of P-TiO_2/TP before and after 10-h electrolysis.

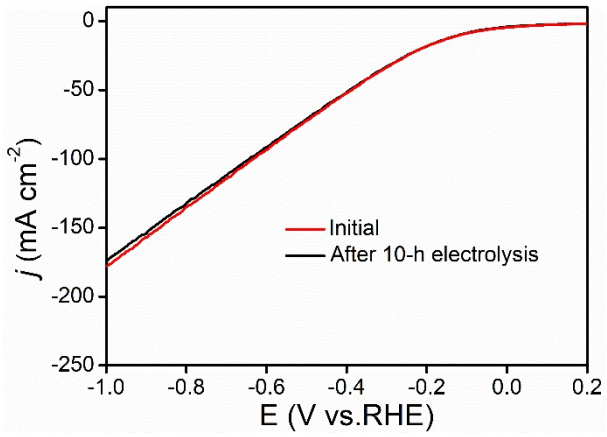

Fig. S16. LSV curves of P-TiO_2/TP before and after 10-h electrolysis.

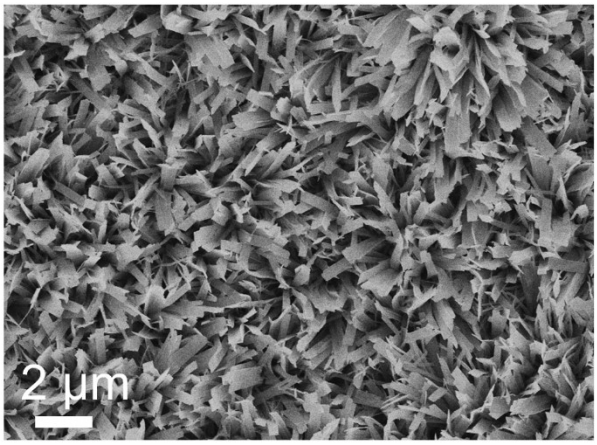

Fig. S17. SEM image of P-TiO_2/TP after 10-h electrolysis.

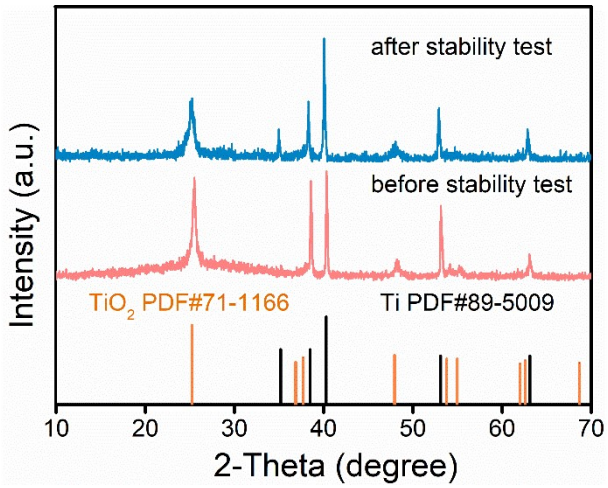

Fig. S18. XRD patterns of P-TiO_2/TP before and after stability test.

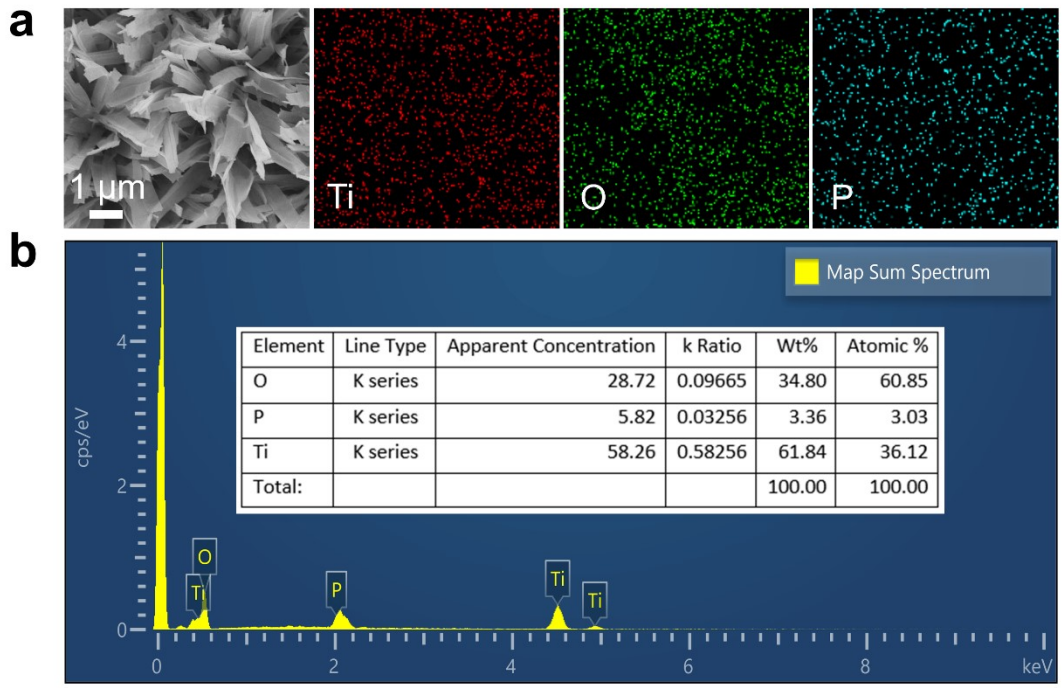

Fig. S19. (a) The SEM and corresponding EDX mapping images of P-TiO_2/TP after 10-h electrolysis. (b) EDX spectrum of P-TiO_2/TP after 10-h electrolysis.

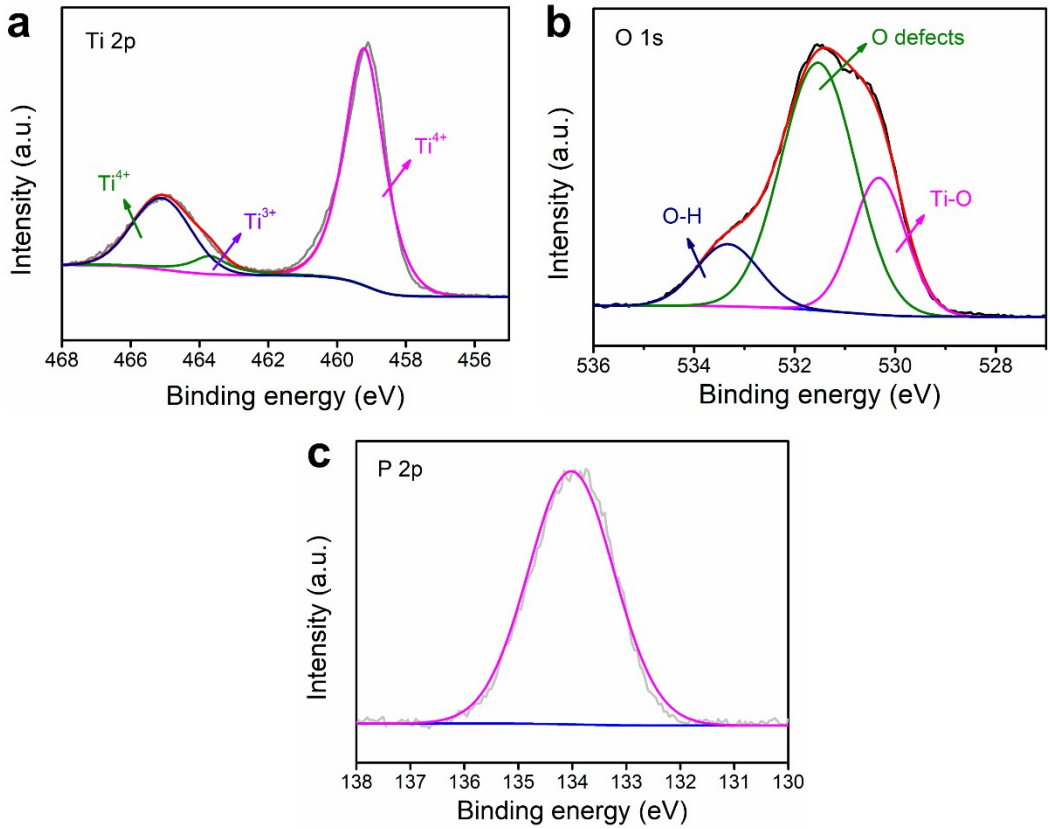

Fig. S20. XPS spectra of (a) Ti 2p, (b) O 1s, and (c) P 2p regions of P-TiO_2 after 10-h electrolysis.

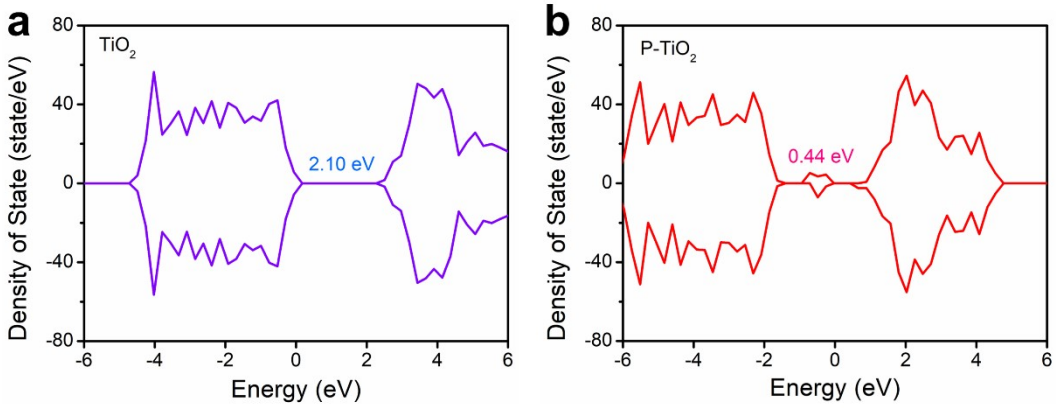

Fig. S21. Electronic density of state of (a) TiO_2 and (b) P-TiO_2. The band gap is labeled.

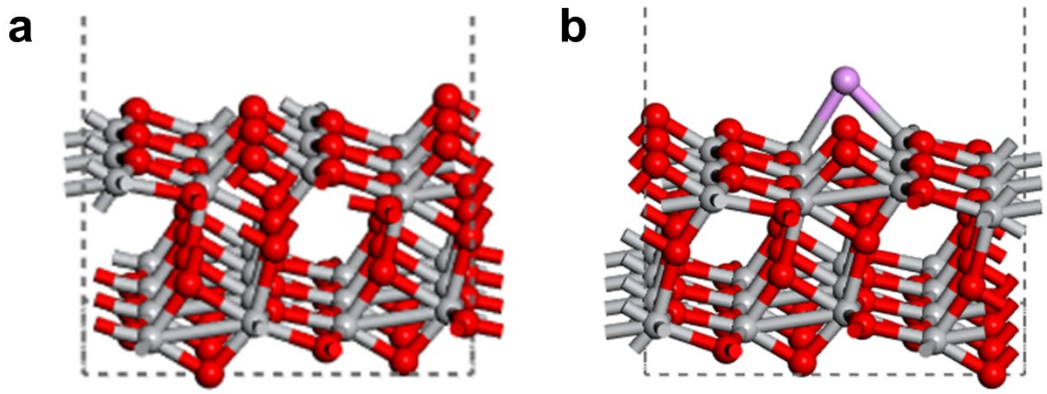

Fig. S22. Relaxed geometry of (a) TiO_2 (101) slab and (b) P-TiO_2 (101) slab.

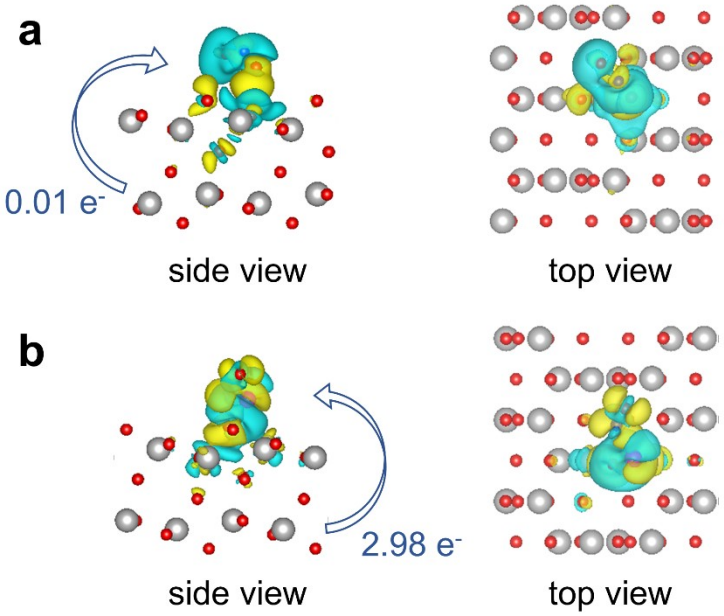

Fig. S23. Electron density difference mappings of *NO_2 on (101) surface for (a) TiO_2 and (b) P-TiO_2. Yellow and green isosurfaces represent electron depletion and accumulation, and gray, red, dark blue, and pink spheres denote the Ti, O, N, and P atoms, respectively.

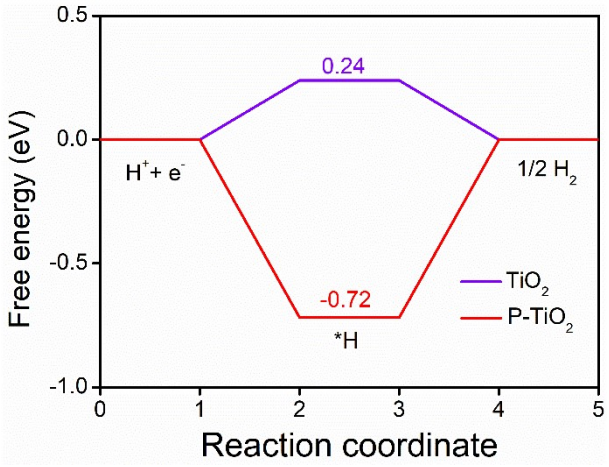

Fig. S24. Free energy diagram of HER on the (101) surface of TiO_2 and P-TiO_2.

Table S1 Comparison of the catalytic performances of P-TiO_2/TP with other reported NO_2^-RR electrocatalysts under ambient conditions.

Catalyst	Electrolyte	NH_3 yield	FE (%)	Ref
P-TiO_2/TP	0.1 M Na_2SO_4 (0.1 M NO_2^-)	560.8 μmol h^{-1} cm^{-2}	90.6	This work
Cu phthalocyanine complexes	0.1 M KOH ($NaNO_2$)	\	78	5
TiO_{2-x} NBA/TP	0.1 M NaOH (0.1 M $NaNO_2$)	464.6 μmol h^{-1} cm^{-2}	92.7	6
Ag@NiO/CC	0.1 M NaOH (0.1 M NO_2^-)	338.3 μmol h^{-1} cm^{-2}	97.7	7
CoP NA/TM	0.1 M PBS (500 ppm $NaNO_2$)	132.9 μmol h^{-1} cm^{-2}	90	8
Cu/JDC/CP	0.1 M NaOH (0.1 M NO_2^-)	523.5 μmol h^{-1} $mg_{cat.}^{-1}$	93.2	9
Ni_2P/NF	0.1 M PBS (200 ppm $NaNO_2$)	191.3 ± 6.6 μmol h^{-1} cm^{-2}	90.2 ± 3.0	10
Anatase TiO_{2-x}	0.1 M NaOH (0.1 M $NaNO_2$)	719.4 ± 23.9 μmol h^{-1} cm^{-2}	91.1 ± 5.5	11
CF@Cu_2O	0.1 M PBS (0.1 M $NaNO_2$)	441.8 μmol h^{-1} cm^{-2}	94.2	12
Cu_3P NA/CF	0.1 M PBS (0.1 M NO_2^-)	95.6 μmol h^{-1} cm^{-2}	91.2	13
Ni-NSA-V_{Ni}	0.2 M Na_2SO_4 (200 ppm $NaNO_2$)	235.98 μmol h^{-1} cm^{-2}	88.9	14
MnO_2 nanoarrays	0.1 M Na_2SO_4 ($NaNO_2$)	235.98 μmol h^{-1} cm^{-2}	6	15

References

1 D. Zhu, L. Zhang, R. E. Ruther and R. J. Hamers, *Nat. Mater*., 2013, **12**, 836–841.

2 G. W. Watt and J. D. Chrisp, *Anal. Chem*., 1952, **24**, 2006–2008.

3 P. E. Blöchl, *Phys. Rev. B.*, 1994, **50**, 17953–17979.

4 J. P. Perdew, K. Burke and M. Ernzerhof, *Phys. Rev. Lett.*, 1996, **77**, 3865–3868.

5 N. Chebotareva and T. Nyokong, *J. Appl. Electrochem.*, 1997, **27**, 975–981.

6 D. Zhao, J. Liang, J. Li, L. Zhang, K. Dong, L. Yue, Y. Luo, Y. Ren, Q. Liu, M. S. Hamdy, Q. Li, Q. Kong and X. Sun, *Chem. Commun.*, 2022, **58**, 3669–3672.

7 Q. Liu, G. Wen, D. Zhao, L. Xie, S. Sun, L. Zhang, Y. Luo, A. A. Alshehri, M. S. Hamdy, Q. Kong and X. Sun, *J. Colloid Interface Sci.*, 2022, **623**, 513–519.

8 G. Wen, J. Liang, Q. Liu, T. Li, X. An, F. Zhang, A. A. Alshehri, K. A. Alzahrani, Y. Luo, Q. Kong and X. Sun, *Nano Res.*, 2022, **15**, 972–977.

9 L. Ouyang, L. Yue, Q. Liu, Q. Liu, Z. Li, S. Sun, Y. Luo, A. A. Alshehri, M. S. Hamdy, Q. Kong and X. Sun, *J. Colloid Interface Sci.*, 2022, **624**, 394–399.

10 G. Wen, J. Liang, L. Zhang, T. Li, Q. Liu, X. An, X. Shi, Y. Liu, S. Gao, A. M. Asiri, Y. Luo, Q. Kong, and X. Sun, *J. Colloid Interface Sci.*, 2022, **606**, 1055–1063.

11 Z. Ren, Q. Chen, X. An, Q. Liu, L. Xie, J. Zhang, W. Yao, M. S. Hamdy, Q. Kong and X. Sun, *Inorg. Chem.*, 2022, 61, 12895–12902.

12 Q. Chen, X. An, Q. Liu, X. Wu, L. Xie, J. Zhang, W. Yao, M. S. Hamdy, Q. Kong and X. Sun, *Chem. Commun.*, 2022, **58**, 517–520.

13 J. Liang, B. Deng, Q. Liu, G. Wen, Q. Liu, T. Li, Y. Luo, A. A. Alshehri, K. A. Alzahrani, D. Ma and X. Sun, *Green Chem.*, 2021, **23**, 5487–5493.

14 C. Wang, W. Zhou, Z. Sun, Y. Wang, B. Zhang and Y. Yu, *J. Mater. Chem. A*, 2021, **9**, 239–243.

15 R. Wang, Z. Wang, X. Xiang, R. Zhang, X. Shi and X. Sun, *Chem. Commun.*, 2018, **54**, 10340–10342.